



Rapid Decolorization of Acid Orange II in Aqueous Solution by Waste Iron Oxide Particles

Md. Abul Kalam Azad¹, Md. Hamidur Rahman¹, Sheikh Jaber Nurani^{1,*},
Md. Abdul Halim^{1,2}, Md. Adnan Karim¹, Fahmida Gulshan¹

¹Department of Materials and Metallurgical Engineering, Bangladesh University of Engineering and Technology, Dhaka-1000, Bangladesh.

²Department of Materials Science and Engineering, King Abdullah University of Science & Technology, Saudi Arabia.

Received 12 Sept 2015, Revised 13 Dec 2015, Accepted 13 Dec 2015

*Corresponding Author. E-mail: sheikh.jaber.nurani@gmail.com; Tel: (+8801771360183)

Abstract

Discharges of highly colored dye effluents in natural water constitute a significant burden on the environment. The solar driven photo-Fenton process based on Fe(III)-oxalate complexes, an important advanced oxidation processes (AOP) technology, has been attracting growing attention for the decomposition of organic dyes. Such processes are based on the light enhanced generation of the highly reactive hydroxyl radicals, which oxidize the organic matter in solution and convert it completely into water, CO₂ and inorganic compounds. In the present study, the effectiveness of iron oxide wastes generated in steel re-rolling mills to decompose a synthesized textile dye named Acid Orange II under UV illuminations was investigated. The decomposition of dye by iron oxide suspension at neutral solution pH was investigated. The experiments were carried out by varying amount of Iron Oxide (IO) catalyst (0.05–1 g/100mL) in Oxalic Acid (OA) concentration of 1mmol/100 mL solution and with initial dye concentration of 0.1 mmol/100mL solution. The optimum catalyst dose was found to be 0.05 g/100mL solution. We also studied the effect of pH and initial dye concentration on the degradation behaviour. From this study it was found that iron oxide wastes could be useful in treating dye wastes thus can play an important role to minimize both iron oxide and dye wastes.

Keywords: Photocatalytic activity, Photo-ferrioxalate process, Acid Orange II.

1. Introduction

Water is an indispensable requirement of life, as well as industries which are working for the betterment of human life and health. Industrialization made a deep impact on human health directly or indirectly creating environment (air, water, soil) polluted by releasing wastes and untreated wastewater, into the environment. In many countries, most of the textile industries are using color materials like dyes and pigments, and effluents are released as a textile effluent to canal, river, and sea without further treatments and purifications. In presence of these organic compounds, water becomes unusable for practical uses. Colorants – dyes and pigments – are a growing pollution problem in the industrial and household wastewater as a result of their extensive use and relative stability towards degradation. Dyes undergo chemical changes as well as biological changes in the aquatic system, consume dissolved O₂ and thus disturb the aquatic eco-system. The untreated dyes in effluents from textile and coloring are a group of hazardous chemicals as well as major sources of water pollution. It is therefore necessary to treat the water containing color dyes and other organic compounds to discharge them.

Due to the complex aromatic structure and stability of these dyes, conventional biological pre-treatment methods are ineffective for degradation. Also low efficiency and low reaction rate are associated with these methods caused the methods to be ineffective. The typical dyestuff treatment includes physical and chemical methods, such as coagulation/flocculation, activated carbon, adsorption and bio-treatment, ozonation, sodium hypochlorite treatment, photochemical decolourization. Amongst the disadvantages of these methods are either formation of large amounts of sludge, or generation of toxic byproducts (aromatic amines) when the

degradation is incomplete, i.e. without the opening of the aromatic ring of the dye molecule. These limitations of conventional wastewater treatment methods can be overcome by the application of the advanced oxidation processes (AOP), which has the unique ability to fully mineralize the dyes, including the opening of the aryl ring.

AOP in a broad sense, refers to a set of chemical treatment procedures designed to remove organic (and sometimes inorganic) materials in water and waste water by oxidation through reactions with hydroxyl radicals ($\bullet\text{OH}$). AOPs such as the Fenton reaction have been found to be very effective for removing organic pollutants from wastewater. The Fenton system involves the generation of $\bullet\text{OH}$ which can degrade most organic compounds to CO_2 and H_2O due to their high oxidation potential ($E_0 = +2.80 \text{ V}$) [1]. In real-world applications of wastewater treatment, however, this term usually refers more specifically to a subset of such chemical processes that employ ozone (O_3), hydrogen peroxide (H_2O_2) and/or UV light to increase the efficiency of $\bullet\text{OH}$ generation [2]. In these reactions, H_2O_2 is added as the direct source of $\bullet\text{OH}$. However, H_2O_2 is an extremely reactive compound and does not survive in nature for long, limiting the usefulness of Fenton and Fenton-like systems for the degradation of organic matter in a natural environment. Other AOPs such as ozonation and ozone related processes ($\text{O}_3/\text{H}_2\text{O}_2$, UV/O_3), heterogeneous photocatalysis (TiO_2/UV), homogeneous photocatalysis (Fenton and Fenton-like processes) and electrochemical oxidation are considered as the most efficient for pesticide degradation in water but these still have not been put into commercial use on a large scale (especially in developing countries) even up to today mostly because of the relatively high costs.

Photophoroxalate system combination of IO and polycarboxylic acids (such as OA) can form a photochemical system to give a photo-Fenton-like reaction without the addition of H_2O_2 , and with much higher quantum efficiency than with $\text{Fe}(\text{OH})^{2+}$ or IO alone [3]. Since the polycarboxylic acids are also abundant in the natural environment, this photochemical oxidation process can directly utilize natural materials (IO and OA) in combination with UV, to decompose organic pollutants economically. It is therefore meaningful to investigate the photodecomposition of organic pollutants in the IO-polycarboxylate complex system to better understand the transformation of organic pollutants [4]. IO is used as catalyst. The structures of the IO are well defined, and particularly interesting, determine the activities for the degradation of organic substrates. IOs are semiconductors with a band gap of 2.2 eV [5]. Thus, it can be photoexcited by light for the decomposition of organic pollutants in waters [6] and the splitting of H_2O to extract hydrogen energy or disinfect the water. Apparently, poorly crystalline IOs release iron ions more readily than their good crystalline counterparts particularly in acidic media. For the photo Fenton reaction, the size of IO particles is an important parameter. The nanosized IOs are stronger absorptive and exhibit improved catalytic activity because of their large surface area which potentially provides more active sites for the generation of $\bullet\text{OH}$ [7]. OA is one of the most active polycarboxylic acids, and has been reported by Li et al. [1], than other carboxylic acids such as citric, tartaric, malonic, malic and succinic acid. The photochemistry of Fe^{3+} -oxalate complexes has been studied by many workers [8] and Fe^{3+} -oxalate complexes are known to exhibit strong ligand-to-metal charge absorption bands in the near-UV and visible region.

During the photochemical reaction of Fe^{3+} -oxalate complexes under UV/sunlight, OA is first adsorbed on the surface of the IO in suspension, forming $[\text{Fe}^{3+}(\text{C}_2\text{O}_4)_n]^{(2n-3)-}$. This complex can then be excited to form $[\text{Fe}^{2+}(\text{C}_2\text{O}_4)_{(n-1)}]^{(4-2n)-}$ and $\bullet\text{C}_2\text{O}_4^-$. Then C_2O_4^- is readily transformed to the carbon-centered radical $\bullet\text{CO}_2^-$ [9], from which the excited electrons are transferred to the adsorbed O_2 , forming superoxide ions $\bullet\text{O}_2^-$. Fe^{3+} can react with $\bullet\text{O}_2^-$ to form O_2 and Fe^{2+} . Then Fe^{2+} reacts with $\bullet\text{O}_2^-$ and $\bullet\text{O}_2\text{H}$ to form H_2O_2 in acidic solution with Fe^{3+} and Fe^{2+} is reoxidized to Fe^{3+} in the presence of O_2 . After H_2O_2 is formed, $\bullet\text{OH}$ can be generated by the reaction of Fe^{2+} with H_2O_2 . The formation of $\bullet\text{OH}$ in the Fe^{3+} -oxalate system and in H_2O_2 has been confirmed by photochemistry [10-11]. The $\bullet\text{OH}$ radicals attack firstly N=N bond and then ring to decompose into inorganic materials [12-13].

In this study, Acid Orange II (AOII) was selected as a model organic pollutant and its degradation studied in the presence of mill scale (waste iron oxides) in oxalate solution under UV illumination.

2. Materials and methods

IO was ball milled to produce fine particles to increase the reactive surface area. The crystalline phases of IO samples were determined by X-ray powder diffraction (XRD) with Monochromatic $\text{CuK}\alpha$ radiation.

The parent solution of AOII of concentration 1M was prepared with distilled water. Solutions of required concentration were then prepared from parent solution for particular experiment. The photodegradation of AOII was carried out using two 8W black light lamps with the main emission at 365 nm. The sample suspension was

formed by adding varying amounts of IO to 100 ml of aqueous solution containing AOII and OA. Before photoreaction, the suspension was magnetically stirred in the dark for 30 minute to establish an adsorption-desorption equilibrium. The various aqueous suspensions were then illuminated by UV while being magnetically stirred. At the given time intervals, the analytical samples were withdrawn from the suspension into a small plastic bottle and then stored in dark for further analysis.

The absorbance spectrum in each experiment was determined from 200 to 600 nm with a UV-Vis spectrophotometer and the degradation of AOII was recorded by monitoring the absorbance intensity of solution samples at their maximum absorbance at $\lambda=484$ nm as a function of illumination time. The photodegradation efficiency of AOII was calculated by using the following formula.

$$\text{Photodegradation efficiency} = \frac{C_0 - C_t}{C_0} \times 100\%$$

Where, C_0 and C_t are initial and final absorbance intensity of AOII solution after time t respectively.

3. Results and discussion

The XRD patterns of the samples were interpreted using ICDD database. The XRD pattern of the sample (Figure 1) collected from steel re-rolling mill, showed major phase of 30.31 % hematite ($\alpha\text{-Fe}_2\text{O}_3$), 41.51 % magnetite (Fe_3O_4) and 29.32 % wustite (FeO).The chemical formula of Acid Orange II is shown in Fig. 2

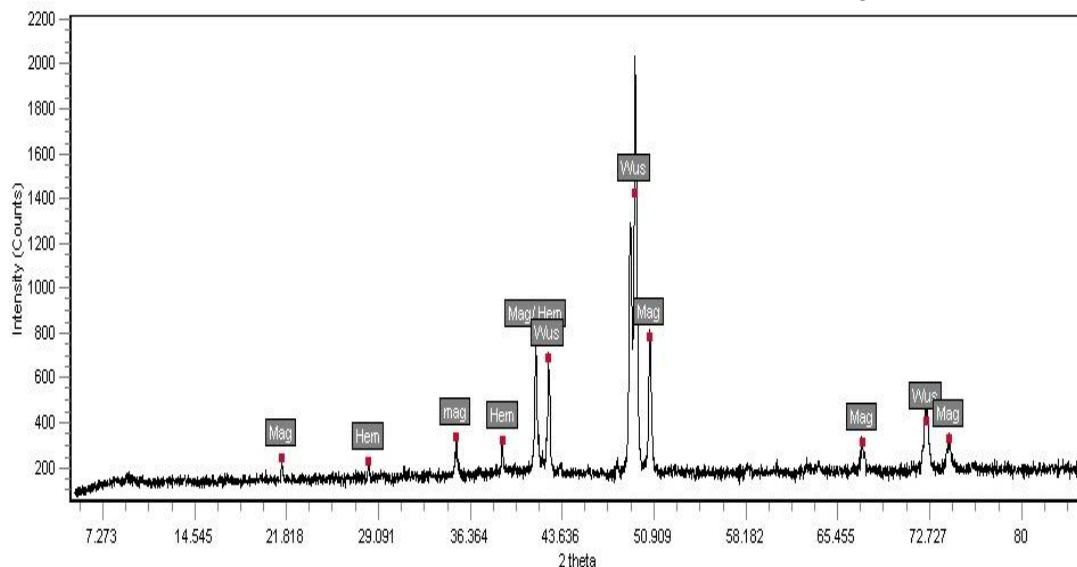


Figure 1: XRD patterns of mill scale.

To determine the wavelength at which maximum absorbance intensity is occurred, absorbance spectra of AOII solution were monitored using UV-Vis spectrophotometer. It is found that AOII has five absorption peaks in which two peaks in visible region and three in ultraviolet region but maximum absorbance occurred at wavelength of 484 nm (Fig. 3). In visible region, a major peak locates at 484nm and a shoulder peak locates at 430nm due to the hydrazone form and azo form of AOII, respectively. The other three peaks in ultraviolet region are assigned to the aromatic ring, among which the peaks at 228nm and 310nm in ultraviolet region are ascribed to the benzene and naphthalene rings of the dye, respectively [11].

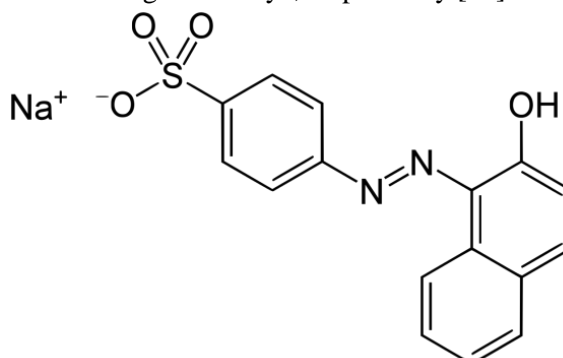


Figure 2: Chemical formula of Acid Orange II

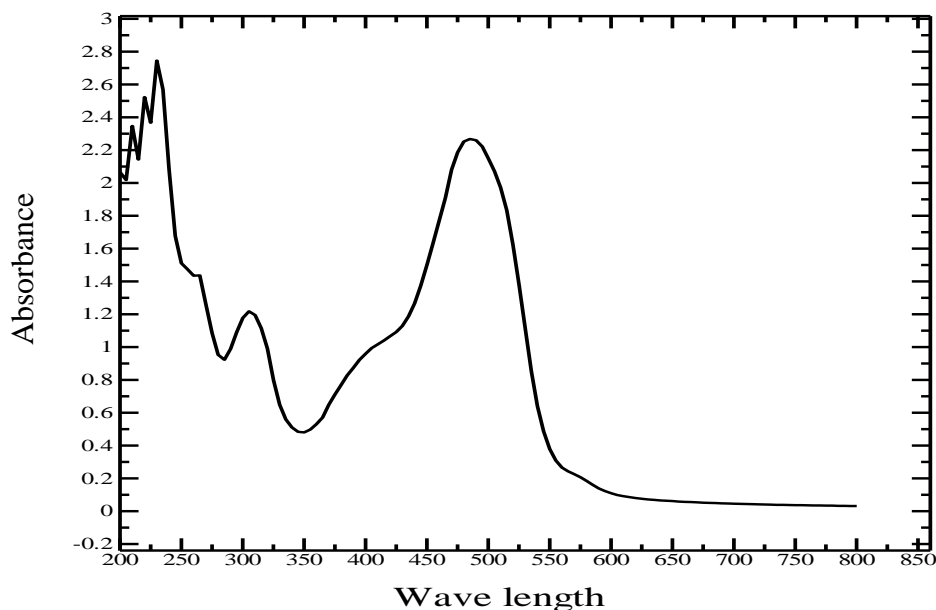


Figure 3: Absorption Spectra of AOII

3.1. Degradation behaviour of AOII

To determine the degradation behaviour of AOII, 1 mmol/100mL dye solution with 1mmol OA and 1g IO was stirred in dark 30 minute and then UV illumination was applied. Here, 1mmol/100mL dye solution is taken as initial dye concentration since it is very optimum and practical for observing the colour change. The samples were collected after 10 minute interval and then absorbance spectra were monitored using UV-Vis spectrophotometer. Absorption peaks at 484nm and 430nm decreased rapidly as the reaction proceeded (Fig. 4) because the $\bullet\text{OH}$ radical firstly attacked azo groups and destructed the N=N bond [11]. And absorption peaks at 310nm and 228nm related to the naphthalene and benzene respectively, gradually decreased.

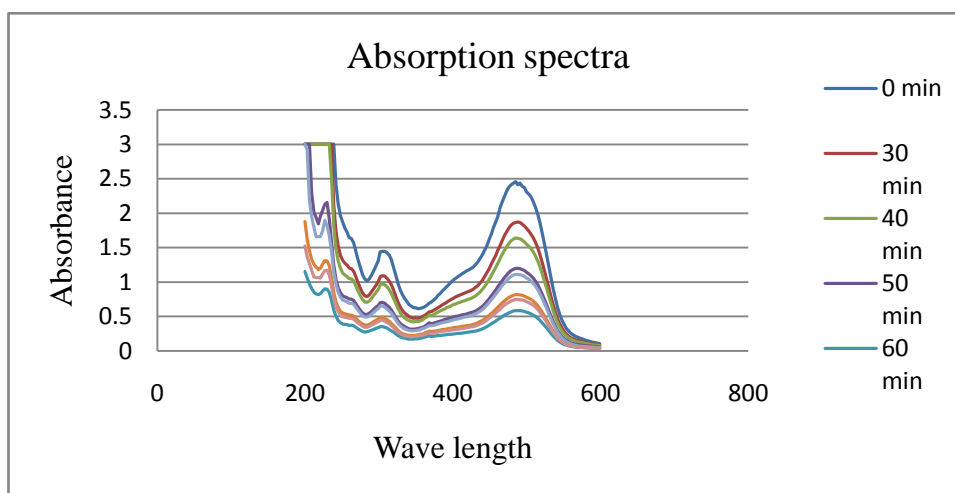


Figure 4. Absorption spectra of AOII showing degradation behavior with time. Reaction condition: [AOII] =1 mmol;[OA]= 1mmol; [IO]= 1g/0.1L; Time = 0-90 minute; Light source= First 30 minute in dark and then UV.

3.2. Effect of Initial Dye Concentration

The effect of initial dye concentration was investigated by varying the initial concentration from 0.01mmol to 0.1mmol using 0.50 gm. of catalyst (iron oxide) and 100 mL of dye solution with 1 mmol oxalic acid under UV illumination for 60 min (first 30 min in dark and then UV). The effect of initial dye concentration is shown in figure 1. It is found that, higher time is required for degradation of higher initial dye concentration 1.

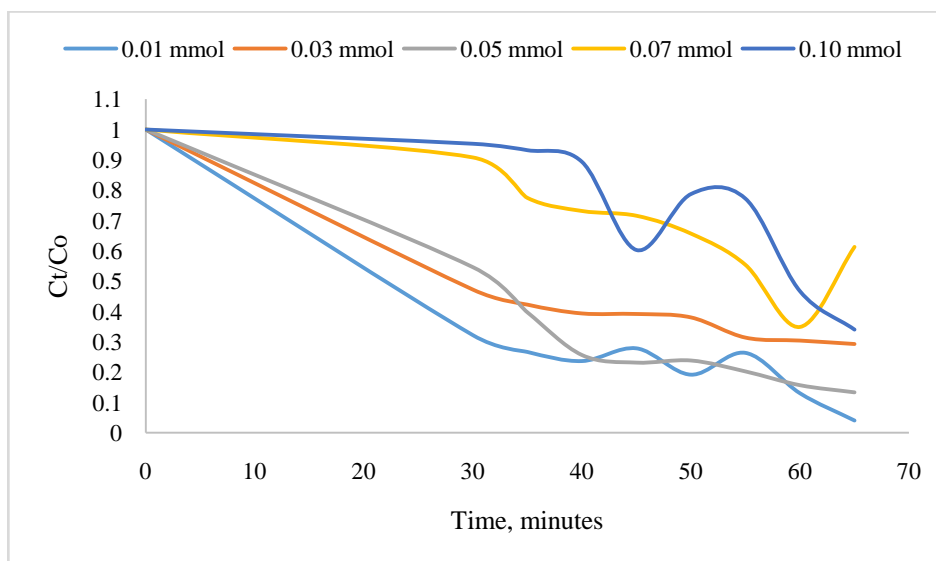


Figure 5. Effect of initial concentration of AOII dye on percentage decolorization. Experimental conditions: [AOII]=0.01mmol to 0.10 mmol; [Mill Scale]=0.5 g/L; Light source: UV; Reaction time: 60min.

The photodegradation efficiency of Acid orange II is inversely proportional to its concentration, which means, the lower of the dye concentration, the higher efficiency of the dye photodegradation (Fig 5). As seen, increasing the initial dye concentration from 0.01mmol to 0.1 mmol decreases the photodegradation efficiency of Acid orange II after 60 minute (first 30 min in dark and then UV Illumination) from 96% to 65.5%. The photodegradation efficiency relates to the formation of hydroxyl radicals, which is the critical species in the degradation process. Hence an explanation to this behavior is that the higher the initial concentration, the higher the adsorbed organic substances on the surface of the catalyst and the solution became more intensely colored.

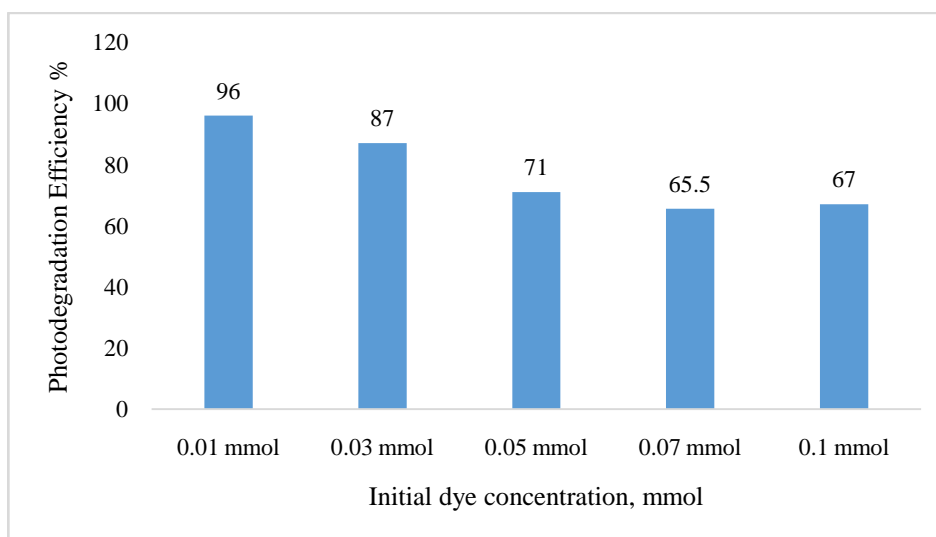


Figure 6. Photodegradation efficiency for different initial concentration of AOII dye. Experimental conditions: [AOII] = 0.01mmol to 0.10 mmol; [IO] = 0.5 g/L; Light source: UV; Reaction time: 60min.

Therefore, there are only fewer active sites for adsorption of HO⁻ so the generation of •HO will be reduced. Furthermore, as the concentration of AOII increases with constant intensity of UV illumination, the path length of photons entering the solution decreased, so only fewer photons reached the catalyst surface. As a result, the productions of holes or hydroxyl radicals that can attack the pollutants were limited. Therefore, the relative number of •HO attaching the compound decreases and thus the photodegradation efficiency decreases [14-16].

3.3. Effect of Various Parameters on Degradation of AOII

100 ml AOII (Co= 0.1 mmol) solution was stirred in dark and no degradation occurred after 1 hour. But while UV illumination was applied, degradation was considerable (Fig. 7) as UV illumination provided activation energy required for bond breaking. After 50 minutes absorbance intensity increased (Fig. 7). It may be due to the experimental errors. Again 100 ml AOII (Co=0.1 mmol) solution with 1 mmol OA was stirred in dark and a little degradation occurred after 35 minute. But while UV illumination was applied, the degradation rate increased rapidly (Fig. 7) since UV illumination provided sufficient energy to break OA to form H₂O₂ and then •OH which enhanced the degradation.

Again 100 ml AOII (Co=0.1mmol) solution with 0.5gm IO was stirred in dark for 30 minutes and then UV illumination was applied. The degradation rate was very much slow in dark but rapidly increased after UV illumination (Fig. 7). The phototreatment (UV illumination) of solid IO can accelerate the recycling of Fe(II)/Fe(III), as illustrated by following equation and produce •OH which degrades AOII [7].



Again 100 ml AOII solution (Co= 0.1 mmol) with 1.0 mmol OA and 0.5 gm IO was stirred in dark. The absorbance intensity decreased up to 30 minutes and then increased and again decreased after 40 minutes (Fig. 7). Sometimes higher absorbance/concentration was noticed due to the intermediaries' formation. But while UV illumination was applied on solution of same concentration and composition, uniform and gradual degradation occurred. Maximum degradation occurred in this case (Fig. 7). Moreover, we can also notice from the Fig. 4 that the intermediaries (if be formed during the degradation process) do not interfere the analysis as there is no peak nearby the absorption intensity $\lambda_{\text{max}}=484\text{nm}$.

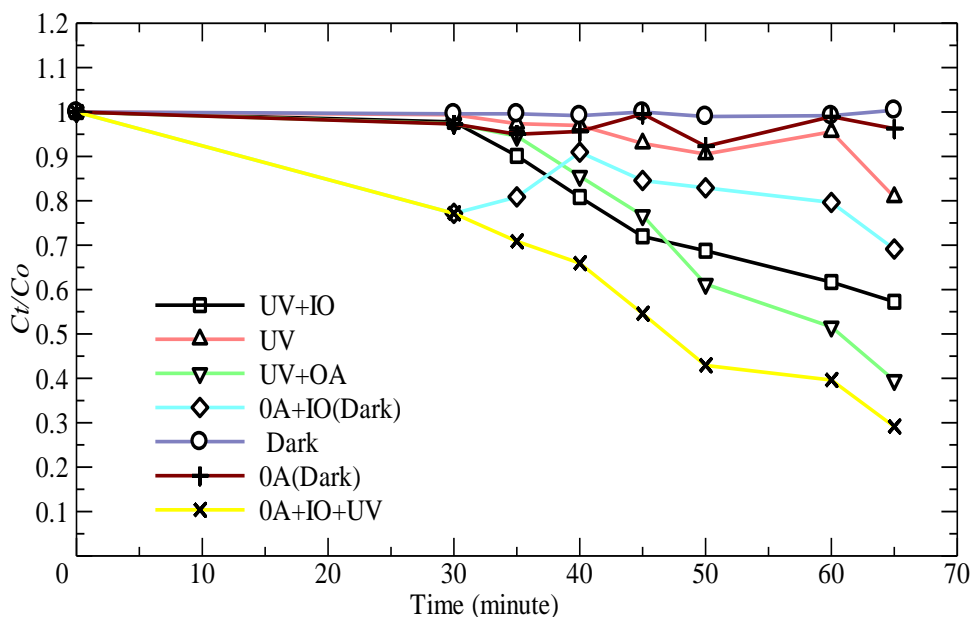


Figure 7. Effect of various parameters (UV, OA, IO and its combination) on degradation of AOII with time.

The degradation efficiency of 0.1 mmol AOII solution is summarized in fig 8.

3.4. Effect of IO Catalyst

To investigate the effect of IO as catalyst, 100 ml AOII (Co = 0.1mmol) solution with 1.0 mmol OA and varying amounts of IO was stirred first in dark for 30 min and then under UV illumination. It was noticed that very low degradation occurred for 0.05 gm IO in dark. But while UV illumination was applied, degradation increased rapidly and highest degradation occurred after 80 minutes (Fig. 9). Because IO acted as catalysts and enhanced •OH production hence increased degradation rate. But with increasing IO content although initial degradation rate was high but actual efficiency decreased. For 0.1 gm IO degradation was considerable in dark and degradation was very high after UV illumination.

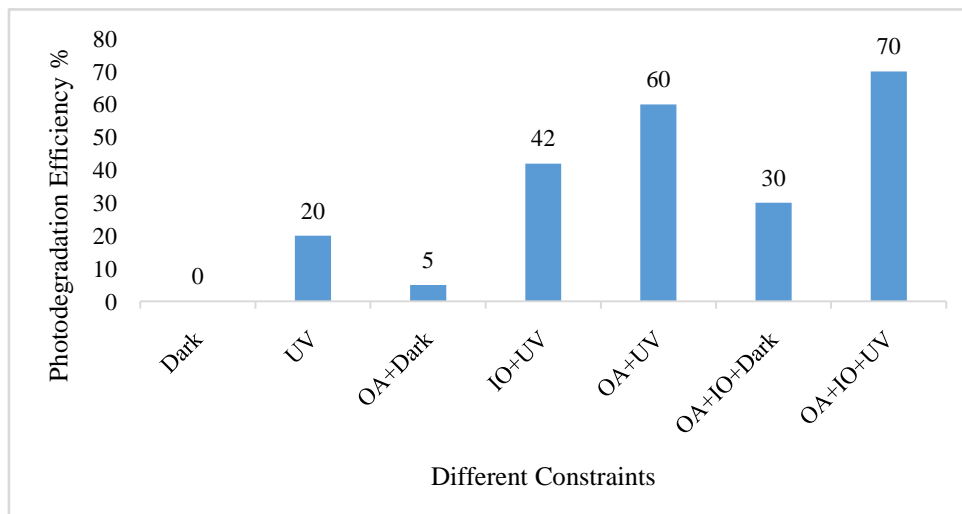
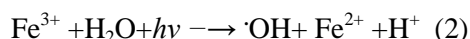


Figure 8. Effect of various parameters (UV, OA, IO and its combination) on degradation of AOII with time.

Hence maximum degradation occurred in short time but overall efficiency was lower than that for 0.05 gm after 80 minutes. For further increasing of IO, though initial degradation was high but actual efficiency was much lower. The overall results are shown in (Fig. 9).

For low IO content, initial degradation rate was lower because it was insufficient to form iron oxalate and then to form $\cdot\text{OH}$. But after UV illumination production of $\cdot\text{OH}$ increased as the following equation [7].



So, this extra $\cdot\text{OH}$ can degrade AOII. But with higher content of IO, degradation becomes lower due to the intermediaries formation. Agglomeration can occur for which active sites for reaction decreases. Also at high amount of catalyst, the opacity, turbidity of the suspension, and light scattering of catalyst particles are increased. This tends to decrease the passage of irradiation through the sample [17]. It is also noticed that absorbance becomes higher than that of previous degraded solution. There may be experimental errors or some new compound formation for which absorbance intensity is high at wavelength of 484 nm. For the degradation of AOII ($\text{Co} = 0.1 \text{ mmol}$) solution with 1 mmol OA, 0.05 gm IO is best suitable.

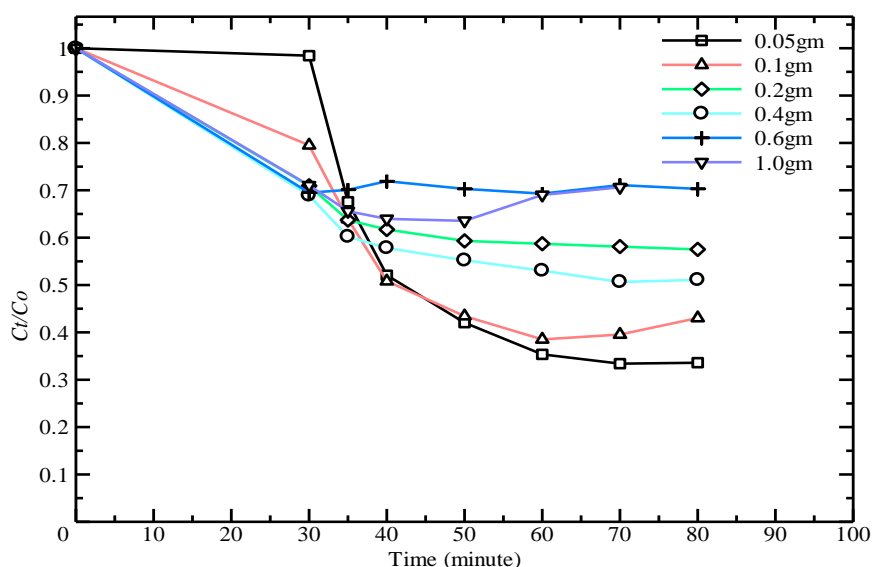


Figure 9. Effect of IO on degradation of AOII with time. Reaction condition: [AOII] = 1 mmol; [OA] = 1mmol; [IO] = 0.5g/0.1L-1.0g/0.1L; Light source= First 30 minute in dark and then UV.

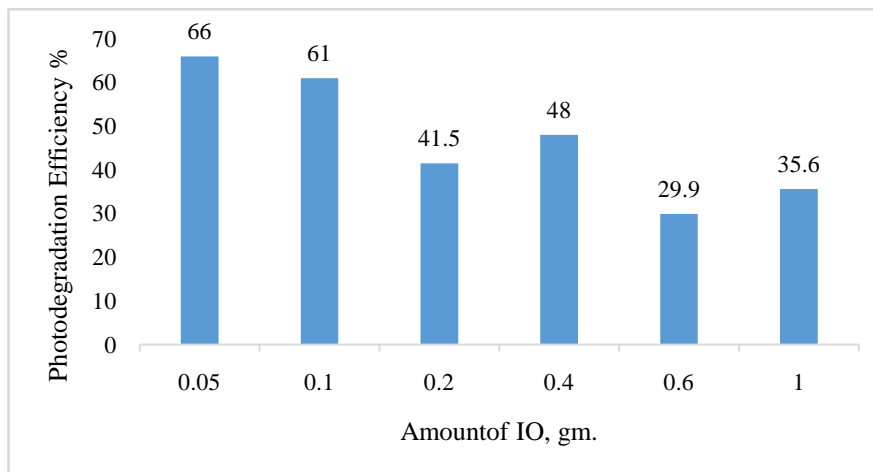


Figure 10. Photodegradation efficiency of AOII. Effect of IO on degradation of AOII with time. Reaction condition: [AOII] = 1 mmol; [OA] = 1 mmol; [IO] = 0.5g/0.1L - 1.0g/0.1L; Light source= First 30 minute in dark and then UV.

The photodegradation efficiency of AOII for various amount of IO with 1 mmol OA was investigated and it was found that the efficiency was highest for 0.05 gm IO for above reaction conditions (Fig. 10). The photodegradation efficiency decreases with increasing IO content. Because excess IO may get agglomerated or occur opacity [7, 18].

3.5. Effect of pH

The effect of pH on the decolorization kinetics has been studied by varying initial pH values. The degree of photodegradation of Acid Orange II in an aqueous Mill Scale suspension for 60 min reaction time in the pH range 3-9 is demonstrated in Fig. 11.

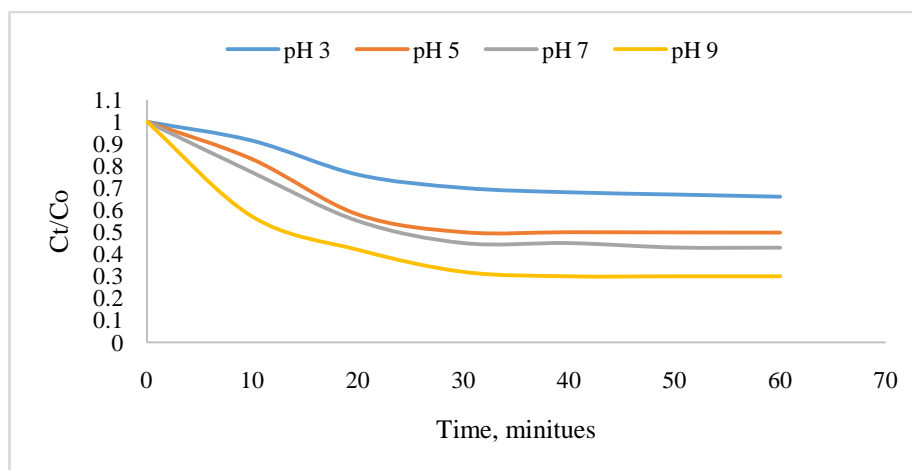


Figure 11. Effect of pH. Reaction condition: [AOII] = 1 mmol; [OA] = 1 mmol; [IO] = 0.5g/0.1L; Light source= First 30 minute in dark and then UV.

The degree of photodegradation increases with increasing pH. Acid base property of the catalytic metal oxide surface dictates the effect of pH on the efficiency of photocatalytic degradation process which can be explained on the basis of zero point charge.

The point of zero charge (PZC) for iron oxide (magnetite, Fe_3O_4) is 6.5-6.8 and for alpha iron oxide (hematite, Fe_2O_3) is 8.4-8.5 [19]. Below and above PZC Iron oxide poses positively charged surface and negatively charged surface by adsorbed OH^- ions respectively. Surface concentration of the dye is relatively high below PZC; as active sites on the positively charged catalyst surface are preferentially covered by dye molecules; while those of OH^- and hydroxyl radical ($\bullet\text{OH}$) are low. The dye molecules cover the catalyst surface and this results in a decreased absorption of UV radiation on the catalyst surface.

Catalyst surface is negatively charged by metal-bound OH⁻ above PZC and surface concentration of the dye is low. The presence of large quantities of OH⁻ ions on the particle surface as well as in the reaction medium favours the formation of OH• radical, which is widely accepted as principal oxidizing species responsible for decolorization process at neutral or high pH levels and results in enhancement of the efficiency of the process [20-22].

Conclusion

The photodegradation of AOII was investigated with varying amounts of IO and with or without UV and AO. For the highest photodegradation efficiency, the combined application of OA, IO and UV illumination is needed. Continuous stirring helps homogenize the solution and facilitate adsorption reaction which enhances the photodegradation efficiency. UV illumination excites IO catalyst and enhance degradation rate. Absorbance/concentration of residual dye solution should be measured instantly as the degradation reaction continues in sunlight even in dark. Degradation rate depends on the amount of IO (catalyst) and its particle size. Finer the particle more is the surface area being exposed for reaction thus increases the process efficiency. Optimization of IO is accomplished with respect to volume and concentration of dye solution. For degradation 100 ml AOII solution (C₀= 0.1mmol) with 1 mmol OA, optimum IO was found to be 0.05 gm.

Acknowledgements-We can't but lay our gratitude to Dr. ASW Kurny, Professor, Department of Materials and Metallurgical Engineering, BUET for her thoughtful suggestion, precious guidance, inspiration, supervision and constant motivation towards the successful completion of our research. We are grateful to other lab coordinators too. The authors admirably acknowledge Bangladesh University of Engineering and Technology for necessary financial contribution and lab facilities.

References

1. Sedlak D.L., Andren A.W., *Environ. Sci. Technol.*, 25 (1991) 1419-1427.
2. Tang W.Z., Chen R.Z., *Chemosphere*, 32 (1996) 947-958.
3. Siffert C., Sulzberger B., *Langmuir*, 7 (1991) 1627-1634.
4. Li F.B., Chen J.J., Liu C.S., Dong J., Liu T.X., *Biol Fertil Soils*, 42 (2006) 409-417.
5. Kay A., Cesar I., Gratzel M., *Journal of the American Chemical Society*, 128 (2006) 15714- 15721.
6. Maji S. K., Mukherjee N., Mondal A., Adhikary B., *Polyhedron*, 33 (2012) 145-149.
7. Wang C., Liu H., Sun Z., *Corporation International Journal of Photoenergy*, 2012 (2012) 1-10.
8. Buxton G.V., Greenstock C.L., Helmen W.P., Ross A.B., *J. Phys. Chem. Ref. Data*, 17 (1988) 513
9. Bandara J., Kiwi J., *New J. Chem.*, 23 (1999) 717-724.
10. Comninellis C., Kapalka A., Malato S., Parson S.A., Poullos I., Mantzavinos D., *Journal of Chemical Technology and Biotechnology*, 83 (2008) 769-776
11. Okhovat N., Hashemi M., Golpayegani A.A., *J. Mater. Environ. Sci.*, 6 (2015) 792-799.
12. Mu Y., Yu H.Q., Zheng J.C., Zhang S.J., *J. Photochem. Photobiol. A*, 163 (2004) 311-316.
13. Zenasni M.A., Meroufel B., Benfarhi S., Merlin A., Molina S., George B., *J. Mater. Environ. Sci.*, 6 (2015) 826-833.
14. Mohamed M.R., Mkhallid I. A., Baeissa E. S., Rayyani M. A., *Journal of Nanotechnology* 2012 (2012) 5.
15. El-Bahy Z. M., Ismail A. A., Mohamed R. M., *Journal of Hazardous Materials*, 166 (2009) 138-143.
16. Ouafi R., Rais Z., Taleb M., Haji M. E., Zemzami M., *J. Mater. Environ. Sci.*, 6 (2015) 1210-1217
17. Liang X., Zhong Y., Zhu S., Zhu J., Yuan P., He H., Zhang J., *Journal of hazardous materials*, 181 (2010) 112-120.
18. Bennani K.A., Mounir B., Hachkar M., Bakasse M., Yaacoubi A., *J. Mater. Environ. Sci.*, 6 (2015) 2483-2500.
19. Kosmulski M., "Chemical Properties of Material Surfaces", *Marcel Dekker*, 2001
20. Roses E., Gonzalez D.E., Lopez C.M., Pineiro A.E., Villaamil E.C., *Bull. Environ. Contam. Toxicol.*, 59 (1997) 210.
21. Akyol A., Yatmaz H.C., Bayramoglu M., *Appl. Catal. B: Environ.*, 54 (2004) 19-24.
22. Mansri A., Bouras B., *Moroccan Journal of Chemistry*, 2 (2014) 252-271.